

# Specific Sterols Required for the Internalization Step of Endocytosis in Yeast

Alan L. Munn,<sup>\*†‡</sup> Antje Heese-Peck,<sup>\*†</sup> Brian J. Stevenson,<sup>\*§</sup> Harald Pichler,<sup>||</sup> and Howard Riezman<sup>\*¶</sup>

<sup>\*</sup>Biozentrum of the University of Basel, CH-4056 Basel, Switzerland; <sup>†</sup>Institute of Molecular Agrobiology, The National University of Singapore, Singapore 117604, Republic of Singapore; and <sup>||</sup>Institut für Biochemie und Lebensmittelchemie, Technische Universität, A-8010 Graz, Austria

Submitted June 28, 1999; Accepted August 12, 1999  
Monitoring Editor: Randy W. Schekman

Sterols are major components of the plasma membrane, but their functions in this membrane are not well understood. We isolated a mutant defective in the internalization step of endocytosis in a gene (*ERG2*) encoding a C-8 sterol isomerase that acts in the late part of the ergosterol biosynthetic pathway. In the absence of Erg2p, yeast cells accumulate sterols structurally different from ergosterol, which is the major sterol in wild-type yeast. To investigate the structural requirements of ergosterol for endocytosis in more detail, several *erg* mutants (*erg2Δ*, *erg6Δ*, and *erg2Δerg6Δ*) were made. Analysis of fluid phase and receptor-mediated endocytosis indicates that changes in the sterol composition lead to a defect in the internalization step. Vesicle formation and fusion along the secretory pathway were not strongly affected in the *ergΔ* mutants. The severity of the endocytic defect correlates with changes in sterol structure and with the abundance of specific sterols in the *ergΔ* mutants. Desaturation of the B ring of the sterol molecules is important for the internalization step. A single desaturation at C-8,9 was not sufficient to support internalization at 37°C whereas two double bonds, either at C-5,6 and C-7,8 or at C-5,6 and C-8,9, allowed internalization.

## INTRODUCTION

Eukaryotic cells are able to internalize extracellular molecules and plasma membrane components via endocytosis (Mellman, 1996; Geli and Riezman, 1998). Endocytic functions include uptake of some nutrients and adaptation to environmental signals by down-regulation of signal receptor molecules present in the plasma membrane. In receptor-mediated endocytosis, a ligand binds specifically to its receptor present in the plasma membrane, leading to the internalization of the ligand–receptor complex into small vesicles (Mellman, 1996; Riezman *et al.*, 1996). Over the past years, genetic approaches in the yeast *Saccharomyces cerevisiae* have greatly aided in the identification and characterization of proteins that function at different stages along the endocytic pathway (Riezman *et al.*, 1996; Geli and Riezman, 1998; Wendland *et al.*, 1998). Of particular interest was the discovery that actin plays a fundamental role in the internalization step in yeast. A requirement for actin has also been reported for endocytosis in animal cells (Parton *et al.*,

1994; Deckert *et al.*, 1996; Lamaze *et al.*, 1997). Various studies revealed that several of the identified yeast proteins have homologous counterparts in animals, and, contrary to previous belief, yeast and animal cells appear to use endocytic machinery that shows at least some mechanistic similarities (Geli and Riezman, 1998). In comparison with some membrane trafficking events, however, the molecular mechanisms underlying endocytosis remain poorly understood.

Over the past years, it has become apparent that in addition to proteinaceous factors, lipids play an important role in endocytosis (Anderson, 1998; Kobayashi *et al.*, 1998). Recent attention has been given to sterols, essential components of cellular membranes in eukaryotic cells. Sterols are mainly present in the plasma membrane (Lange, 1991; Zinser *et al.*, 1993), and this localized concentration may reflect a specific function of sterols in this membrane. In animal cells, the major sterol is cholesterol (Lange, 1991). Based on the raft hypothesis, cholesterol is proposed to interact with sphingolipids to form lipid microdomains or so-called lipid rafts that serve as platforms for many cellular events such as membrane trafficking and signal transduction (Simons and Ikonen, 1997; Brown and London, 1998). For membrane trafficking, these lipid rafts may be involved in the lateral recruitment and subsequent internalization of specific proteins (Harder and Simons, 1997; Brown and London, 1998).

<sup>†</sup> These authors contributed equally to this work.

<sup>§</sup> Present address: Novartis Pharma AG, CH-4002 Basel, Switzerland.

<sup>¶</sup> Corresponding author. E-mail address: riezman@ubaclu.unibas.ch.

Studies using drugs that sequester cholesterol or block sterol biosynthesis at an early step in the biosynthetic pathway support a role of cholesterol in endocytosis in animal cells. Depletion for cholesterol leads to a loss of invaginated caveolae and caveolae-like domains (Rothberg *et al.*, 1990; Rothberg *et al.*, 1992; Schnitzer *et al.*, 1994; Hailstones *et al.*, 1998) and to a flattening of clathrin-coated pits (Rodal *et al.*, 1999; Subtil *et al.*, 1999). Furthermore, it inhibits internalization of proteins, including the bacterial cholera toxin (Orlandi and Fishman, 1998), the transferrin-receptor (Rodal *et al.*, 1999) and glycosylphosphatidylinositol-anchored proteins such as the folate receptor, alkaline phosphatase, and CD59 (Chang *et al.*, 1992; Cerneus *et al.*, 1993; Deckert *et al.*, 1996).

In yeast, it is unknown whether sterols serve a similar function in endocytosis. The major sterol of yeast is ergosterol, which, like cholesterol, is mainly present in the plasma membrane (Zinser *et al.*, 1993). Mammalian cells can acquire cholesterol either by endogenous biosynthesis or by internalization of extracellular sterols via receptor-mediated endocytosis or receptor-mediated transfer (Fielding and Fielding, 1997). In contrast, yeast relies only on endogenous ergosterol biosynthesis. They are unable to take up sterols from the extracellular medium under aerobic growth conditions (Trocha and Sprinson, 1976; Keesler *et al.*, 1992). Most *ERG* genes of the ergosterol biosynthetic pathway are essential, and only five proteins functioning in the final steps of the pathway are encoded by nonessential *ERG* genes (Lees *et al.*, 1995; Parks and Casey, 1995; Daum *et al.*, 1998). Thus, yeast cells containing *erg* mutations in the late part of the biosynthetic pathway are viable but are unable to synthesize ergosterol. Each *erg* mutant accumulates, however, a distinct set of sterols that differ from ergosterol in specific structural features, thus leading to changes in the membrane composition (Lees *et al.*, 1995). In yeast, two functions of ergosterol have been examined in more detail, the so-called "sparking function" and the bulk membrane function. For the sparking function, sterols in nanomolar concentrations are required for yeast cells to complete the cell cycle. Only sterols with specific structural features are sufficient to overcome this cell cycle arrest in the G1 to S transition (Rodriguez and Parks, 1983; Lorenz *et al.*, 1989). In contrast, a number of sterols can fulfill the bulk membrane function in yeast (Nes *et al.*, 1993). This function is important for modulating the fluidity and permeability of the plasma membrane. Changes in the sterol composition have been reported to increase or decrease the sensitivity of the yeast cell to certain drugs (Lees *et al.*, 1995; Parks and Casey, 1995), to decrease the activity of plasma membrane proteins (Gaber *et al.*, 1989; Welihinda *et al.*, 1994), and to decrease cell-cell fusion during mating (Gaber *et al.*, 1989; Tomeo *et al.*, 1992). Overall, however, the physiological roles of sterols in yeast remain largely unknown.

In the present studies, we show that ergosterol is required for the internalization step of endocytosis in yeast. Previously, the *end11-1* mutant was isolated in a genetic screen for yeast mutants defective in endocytosis (Munn and Riezman, 1994). Analysis of fluid phase and receptor-mediated endocytosis demonstrated that *end11-1* is defective in the first step of endocytosis, the internalization step (Munn and Riezman, 1994). It also exhibits a reduced growth rate at 24 and 37°C. We report here that *END11* is allelic to *ERG2*, a gene that encodes the C-8 sterol isomerase that acts in the late part

of the ergosterol biosynthetic pathway (Arthington *et al.*, 1991). Erg2p converts fecosterol to episterol by isomerizing a C-8,9 double bond to a C-7,8 double bond in the B ring of the sterol molecule (Figure 1). Yeast strains containing mutations in the *ERG2* gene lack the C-8 sterol isomerase activity and are not able to synthesize ergosterol (Arthington *et al.*, 1991). They accumulate sterols different from ergosterol that lack the double bond at C-7,8. The identification of *END11* as *ERG2* indicates that sterols different from ergosterol may not be able to support endocytosis in yeast. To gain a better understanding of how the endocytic defect correlates with changes in the sterol composition, we analyzed endocytosis in *erg* mutants (*erg2Δ*, *erg6Δ*, and *erg2Δerg6Δ*) known to synthesize different sets of sterols. Erg6p is the C-24 sterol methyltransferase that acts immediately upstream of Erg2p in the ergosterol biosynthetic pathway (Gaber *et al.*, 1989; Figure 1). In contrast to Erg2p, Erg6p modifies the side chain of the sterol molecule by methylating zymosterol at the C-24 position to produce fecosterol (Gaber *et al.*, 1989; Figure 1). Thus, *erg6Δ* mutant strains have been reported to accumulate sterols lacking proper side chain modifications. The *erg2Δerg6Δ* double mutant strain lacks both C-8 sterol isomerase and C-24 sterol methyltransferase activities and has been reported to accumulate mainly zymosterol (Bard *et al.*, 1977). When compared with ergosterol, zymosterol lacks both a proper B ring desaturation as well as a proper side chain modification (Figure 1). Analysis of these *ergΔ* mutants allowed us to correlate the endocytic defects with the sterol composition of each *ergΔ* mutant. Our work highlights the importance of specific structural features present in the ergosterol molecule for the internalization step of endocytosis in yeast.

## MATERIALS AND METHODS

### Media and Strains

Yeast strains used in this study are listed with the relevant genotypes in Table 1. SD selective medium and YPUATD medium were prepared as described by Munn *et al.* (1995), except that 40 μg/ml tryptophan were added to YPUAD after autoclaving. Where specified, nystatin (Life Technologies, Paisley, United Kingdom) was added to SD complete medium at a final concentration of 33 U/ml. Plasmid propagation was carried out in *Escherichia coli* strain DH5α (Sambrook *et al.*, 1989). Bacterial strains were grown in Luria-Bertani medium containing 100 μg/ml ampicillin where necessary to select for plasmids (Sambrook *et al.*, 1989). All solid media for growth of yeast and bacteria contained 2% Bactoagar (Difco, Detroit, MI).

### Yeast Genetic Techniques and DNA Manipulations

Mating of haploid strains of yeast, sporulation of diploid strains, and tetrad dissection were performed generally as described in Sherman *et al.* (1974). A Leitz (Wetzlar, Germany) micromanipulator attached to a microscope with fixed stage (Wild, Heerbrugg, Switzerland) was used for tetrad dissection. The plasmids used in this study are shown in Table 1. The lithium acetate method of yeast cell transformation was used for introduction of plasmids into yeast cells (Gietz *et al.*, 1992; Munn *et al.*, 1995). Plasmids were recovered from yeast cells by the method of Ward (1990). Standard molecular procedures were performed according to the methods of Sambrook *et al.* (1989).

### Cloning of the Wild-Type *END11* Gene

An *S. cerevisiae* genomic library constructed in the *LEU2*-marked centromere vector YCplac111 (Gietz and Sugino, 1988; constructed

**Table 1.** Strains and plasmids used in this study

Strain/plasmid	Genotype/description	Source
<b>Strains</b>		
RH448	<i>MATa his4 leu2 ura3 lys2 bar1</i>	Lab strain
RH1201	<i>MATα/MATa his4/his4 leu2/leu2 ura3/ura3 lys2/lys2 bar1/bar1</i>	Lab strain
RH1737	<i>MATa his4 leu2 ura3 bar1 sec18</i>	Lab strain
RH1800 (RH144-3D)	<i>MATa his4 leu2 ura3 bar1</i>	Lab strain
RH1894 (RH296-10D)	<i>MATα his4 ura3 erg6Δ</i>	Lab strain
RH2622 (RH522-2C)	<i>MATa his4 leu2 ura3 ade6? lys2? bar1 end11(erg2)-1</i>	Lab strain
RH2635 (RH144-3A)	<i>MATα his4 leu2 ura3 bar1</i>	Lab strain
RH2180 (SF838-9D vps1-Δ2)	<i>MATα his4 leu2 ura3 ade6 pep4 ops1-Δ2::LEU2</i>	T. Stevens
RH2894 [RH144-3A <i>ERG2(END11)::URA3</i> ]	<i>MATα his4 leu2 ura3 bar1 ERG2(END11)::URA3</i>	This study
RH2895 (RH2894 × RH2622)	<i>MATα/MATa his4/his4 leu2/leu2 ura3/ura3 ADE6/ade6? LYS2/lys2? bar1/bar1 end11(erg2)-1/ERG2(END11)::URA3</i>	This study
RH2896 [RH1201 <i>erg2(end11)-Δ1::URA3</i> ]	<i>MATα/MATa his4/his4 leu2/leu2 ura3/ura3 lys2/lys2 bar1/bar1 erg2(end11)-Δ1::URA3/ERG2(END11)</i>	This study
RH2897	<i>MATa his4 leu2 ura3 lys2 erg2(end11)-Δ1::URA3 bar1</i>	This study
RH2878 (RH407-1B)	<i>MATa his3 leu2 ura3 ade2 lys2 bar1</i>	Lab strain
RH3610 (RH1894 × RH2897, 559)	<i>MATα/MATa his4/his4 leu2/LEU2 ura3/ura3 lys2/LYS2 erg2(end11)-Δ1::URA3/ERG2(END11) erg6Δ/ERG6 bar1/bar1?</i>	This study
RH3611 (RH559-8A)	<i>MATα his4 ura3 erg6Δ erg2(end11)-Δ1::URA3 bar1?</i>	This study
RH3612 (RH559-9B)	<i>MATα his4 ura3 erg2(end11)-Δ1::URA3 erg6Δ bar1?</i>	This study
RH3614 (RH3612 × RH2878, 562)	<i>MATα/MATa his4/HIS4 leu2/LEU2 ura3/ura3 his3/HIS3 ade2/ADE2 lys2/LYS2 bar1/bar1? erg2(end11)-Δ1::URA3/ERG2(END11) erg6Δ/ERG6</i>	This study
RH3616 (RH562-8D)	<i>MATa leu2 ura3 erg2(end11)-Δ1::URA3 erg6Δ bar1</i>	This study
RH3617 (RH562-1A)	<i>MATa his (his3, his4, or his3 his4) ura3 erg2(end11)-Δ1::URA3 erg6Δ bar1</i>	This study
RH3622	<i>MATa his4 leu2 ura3 erg6Δ::LEU2 bar1</i>	This study
<b>Plasmids</b>		
pBluescript KS–YCplac111	ApR <i>E. coli</i> cloning vector ApR, LEU2-marked CEN/ARS <i>E. coli/S. cerevisiae</i> shuttle vector	Stratagene Gietz and Sugino, 1988
Ylplac211	ApR, URA3-marked <i>S. cerevisiae</i> integration vector	Gietz and Sugino, 1988
pEND11.2	YCplac111 genomic library plasmid carrying <i>ERG2(END11)</i> on a 6.3-kb partial- <i>Sau3A</i> fragment	This study
pBKS-END11	2.9-kb <i>Bam</i> HI fragment containing <i>ERG2(END11)</i> in pBKS	This study
Ylplac211- <i>ERG2</i>	2.9-kb <i>Bam</i> HI fragment containing <i>ERG2(END11)</i> in Ylplac211	This study
pend11-Δ1::URA3	pBKS-END11 in which the <i>Bg</i> III- <i>Sph</i> I fragment extending from nucleotides –110 to +495 relative to the start of <i>ERG2(END11)</i> was replaced by a 1.1-kb <i>Bam</i> HI fragment containing URA3	This study
pIU222	YCp50 carrying a copy of <i>ERG6</i> in which an internal 400bp <i>Xba</i> I- <i>Sa</i> II fragment was replaced by the wild-type LEU2 gene	Gaber <i>et al.</i> , 1989

and kindly provided by Fatima Cvrckova, Institute of Molecular Pathology, Vienna, Austria) was transformed into the *end11-1* mutant (RH2622). *Leu*<sup>+</sup> transformants were selected at 24°C. Approximately 1 × 10<sup>5</sup> transformant colonies were pooled and replated at 37°C on SD selective medium to select for temperature-resistant growth. *Leu*<sup>+</sup> transformants that displayed improved growth on SD selective medium at 37°C were chosen for further analysis. Plasmids were isolated from five yeast transformants, amplified in *E. coli* strain DH5α, and reintroduced into the *end11-1* mutant strain. One plasmid showed a reproducible ability to restore wild-type growth at 37°C to cells carrying the *end11-1* mutation. This plasmid contained an insert of 6.3 kb and was named pEND11.2. The minimal DNA insert required for complementation of the *end11-1* growth defect was identified as a 1.2-kb *Pst*I-*Kpn*I fragment by creating various deletions at the left and right ends of the insert and testing the deleted clones for complementation of the growth defect of *end11-1*. DNA sequence analysis of the 1.2-kb *Pst*I-*Kpn*I fragment revealed an open read-

ing frame encoding a protein of 222 amino acids. Comparison with sequences in the nonredundant protein database showed that the identified gene is *ERG2*, which encodes C-8 sterol isomerase (Arthington *et al.*, 1991).

To test whether *ERG2* is the locus affected in *end11-1* mutants or an unlinked gene that can suppress *end11-1*, the cloned *ERG2* gene was tagged with *URA3* to perform integrative mapping of the *URA3*-tagged *ERG2* gene and *end11-1*. A 2.9-kb *Bam*HI fragment carrying the complete *ERG2* gene was cloned from pEND11.2 into the integration vector Ylplac211 (marked with *URA3*; Gietz and Sugino, 1988) to create Ylplac211-*ERG2*. The tagged *ERG2* construct was integrated into the genome of a haploid wild-type strain (RH2635) at the chromosomal locus corresponding to the cloned DNA sequence to create RH2894. RH2894 was crossed to the *end11-1* haploid RH2622 to create the diploid strain RH2895. Consistent with the tagged *ERG2* locus being tightly linked to *end11-1*, all *Ura*<sup>+</sup> haploids derived from RH2895 were nystatin sensitive (*END11*) and all *Ura*<sup>–</sup> haploids were nystatin resistant (*end11-1*).



## DNA Sequence Analysis

For DNA sequence analysis, inserts were subcloned into pBluescript KS II or pBluescript SK II vectors (Stratagene, La Jolla, CA). Double-stranded DNA was prepared and denatured with sodium hydroxide treatment before primer annealing using a modification of the method of Chen and Seeburg (1985). DNA sequencing was carried out with a Sequenase II kit according to the manufacturer's specifications (United States Biochemical, Cleveland, OH). Reactions were resolved by electrophoresis using a Sequi-Gen DNA Sequencing Cell (Bio-Rad, Hercules, CA). DNA sequences were analyzed using the University of Wisconsin (Madison, WI) Genetics Computer Group programs run on a VAX/VMS computer system at the Universität Rechnung Zentrum at the University of Basel.

## Construction of *erg* Deletion Alleles

To disrupt the *ERG2/END11* gene, the 2.9-kb *Bam*HI fragment from pEND11.2, which contains the entire open reading frame, was subcloned into pBluescript KS- (Stratagene) to create pBKS-END11. The *Bgl*III-*Sph*I fragment extending from nucleotides -110 to +495 relative to the start of translation of *ERG2* was then replaced by a 1.1-kb *Bam*HI fragment containing *URA3* to generate p $\Delta$ 11- $\Delta$ 1::URA3. During the cloning, the *Bam*HI sites flanking *URA3* were destroyed by base filling and blunt-end ligation, leaving only the outer *Bam*HI sites. Digestion of p $\Delta$ 11- $\Delta$ 1::URA3 with *Bam*HI releases a *URA3* fragment with *ERG2/END11*-flanking sequences. This fragment was used for disruption of *ERG2/END11* in the homozygous wild-type diploid strain RH1201. Sporulation of the heterozygous diploid strain (RH2896) generated by the disruption event yielded *Ura*<sup>+</sup> recombinant haploid spores in which the *ERG2/END11* locus was deleted [*erg2(end11)* $\Delta$ 1::URA3]. The strain RH2897 is derived from a spore of RH2896. The *ERG6* gene was disrupted in RH1800 using the *erg6* $\Delta$ ::*LEU2* construct pIU222 (Gaber *et al.*, 1989).

The strain RH1894 contains an unmarked disruption of the *ERG6* gene (*erg6* $\Delta$ ). It is a *MAT* $\alpha$  *erg6* $\Delta$  haploid derived from a cross of MD59 to RH1800. To create an *erg2* $\Delta$ *erg6* $\Delta$  heterozygous double mutant strain (RH3610), RH2897 was crossed to RH1894. After sporulation of RH3610, tetrads were dissected onto YPUATD solid medium and incubated at 24°C. Most presumed double mutant spores were inviable, but two *MAT* $\alpha$  double mutant spores survived of 16 tetrads (64 spores) dissected (RH3611 [8A] and RH3612 [9B]; see Figure 2). These spores gave rise to extremely slow-growing colonies. RH3612 was then crossed to the wild-type strain RH2878 to create the diploid RH3614. RH3614 was sporulated, and tetrads were dissected. Two mutations conferring nystatin-resistance segregated in this cross, consistent with RH3612 being a true *erg2* $\Delta$ *erg6* $\Delta$  double mutant. Two viable *MAT* $\alpha$  haploids arising from the RH3614 diploid, RH3616 and RH3617, were of presumed genotype *erg2* $\Delta$ *erg6* $\Delta$  and were retained. Like RH3611 and RH3612, RH3616 and RH3617 also grew extremely slowly. In crosses of RH3616 and RH3617 to the wild-type *MAT* $\alpha$  strain RH2635, two mutations conferring nystatin resistance were segregating. This is consistent with RH3616 and RH3617 having the genotype *erg2* $\Delta$ *erg6* $\Delta$ . For reasons we do not understand, in these crosses most of the *erg2* $\Delta$ *erg6* $\Delta$  double mutant spores were viable (but formed tiny colonies).

## Endocytosis Assays

For fluid phase endocytosis assays, cells were incubated with Lucifer yellow carbohydrazide (LY, dilithium salt; Fluka, Buchs, Switzerland) in YPUATD medium for 1 h at 24°C, washed, examined microscopically, and photographed as described by Munn and Riezman (1994). The [<sup>35</sup>S] $\alpha$ -factor was prepared as described by Munn and Riezman (1994).  $\alpha$ -Factor uptake and degradation assays were performed on cells grown at 24°C to a final density of 0.7–1.0  $\times$  10<sup>7</sup> cells/ml in YPUATD medium. The internalization assays were carried out at 24 or 37°C using the continuous presence protocol with

a 15-min preshift to the respective temperatures before adding the [<sup>35</sup>S] $\alpha$ -factor (Dulic *et al.*, 1991). Internalization (in percentage) was calculated by dividing internalized counts (pH1-resistant counts) by the total cell-associated counts (pH6-resistant counts) for each time point. Values correspond to the means of three or four experiments. For  $\alpha$ -factor degradation assays, [<sup>35</sup>S] $\alpha$ -factor was allowed to pre-bind to cells on ice for 50 min. Subsequent incubation was at 37°C. Samples were taken at times indicated and diluted in pH1 (internalized counts) or pH6 (total cell-associated counts) buffer. Subsequent cell extractions and separation of intact from degraded radiolabeled  $\alpha$ -factor were done as described by Dulic *et al.* (1991).

## Carboxypeptidase Y Delivery to the Vacuole

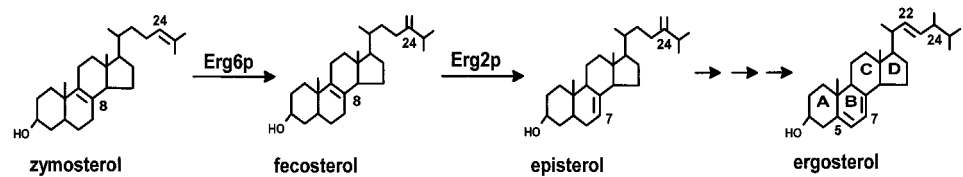
Cells were grown in SD containing 0.2% yeast extract at 24°C to an A<sub>600</sub> of 0.5–1.0. Then 20 A<sub>600</sub> units of cells were harvested, washed in SD, and resuspended in 2.5 ml of fresh SD (preheated to 37°C). After 15 min of incubation at 37°C, the cells were metabolically labeled with [<sup>35</sup>S]methionine and [<sup>35</sup>S]cysteine (Tran<sup>35</sup>S-label or EASYTAG EXPRESS protein labeling mix <sup>35</sup>S; New England Nuclear, Boston, MA) at 37°C for 5 min and chased with unlabeled methionine, cysteine, and sulfate as described by Munn *et al.* (1995). At 0, 5, 10, and 30 min after addition of the chase, samples were removed to microfuge tubes on ice containing sodium azide and sodium fluoride (20 mM final concentration each). The cells were collected by centrifugation and directly lysed by agitation in 500  $\mu$ l of 2% SDS with 0.5 g of 0.5-mm-diameter glass beads. After heating the lysates immediately to 90°C, the debris were sedimented by centrifugation. The cleared supernatants were subjected to immunoprecipitation with carboxypeptidase Y (CPY)-specific antibodies followed by protein A-Sepharose (Pharmacia, Uppsala, Sweden). After washing several times in TNET (100 mM Tris-HCl, pH 8, 100 mM NaCl, 5 mM EDTA, 1% Triton X-100) and once in 20 mM Tris-HCl, pH 7.5, the immunoprecipitates were dissolved in 2 $\times$  Laemmli sample buffer (Laemmli, 1970) and heated to 90°C for 3 min. Immunoprecipitates were resolved on 7.5% SDS-polyacrylamide gels (Laemmli, 1970). The gels were dried, and the radiolabeled CPY was visualized with a PhosphorImager (Molecular Dynamics, Sunnyvale, CA).

Secretion of p2 CPY was examined using the colony immunoblotting assay described by Rothman *et al.* (1986). The extremely slow-growing *erg2* $\Delta$ *erg6* $\Delta$  strain was patched onto a YPUATD plate and incubated for 1 d at 24°C. Then the other strains to be tested were patched onto the YPUATD plate and grown for an additional 1 d. The plate was then overlaid with a nitrocellulose filter (BA85, 0.45  $\mu$ m; Schleicher & Schuell, Dassel, Germany) and incubated for an additional 1 d at 24°C to allow the yeast patches to grow to the same density. The nitrocellulose filter was removed, and cells were eluted from the filter by several distilled water washes. The filter was blocked in 2% skim milk, 1 $\times$  PBS, and 0.1% Tween 20 for 1–2 h and probed with a rabbit polyclonal antiserum against CPY or calmodulin followed by goat anti-rabbit immunoglobulin G coupled to horseradish peroxidase (Bio-Rad). After several washes with PBS, the presence of p2 CPY antigen on the filter was visualized by using an enhanced chemiluminescence kit (Amersham, Arlington Heights, IL) and XAR x-ray film (Kodak, Rochester, NY).

## Invertase Secretion Assays

The invertase secretion assays were performed according to the methods of Novick and Schekman (1979) with some modifications. Yeast cells were grown at 24°C to an A<sub>600</sub> of 0.2–0.5 in YPUATD medium. Ten A<sub>600</sub> units of cells were harvested, washed in distilled water, and induced for invertase expression by resuspension in YPUAT(low D)S medium (containing 0.05% glucose and 2% sucrose) prewarmed to 37°C. Cell samples were taken after 0, 15, 30, 45, and 60 min of induction at 37°C. Membrane transport was blocked by addition of sodium azide to 10 mM final concentration and transfer to ice. Cells of each sample were washed twice in ice-cold 10 mM sodium azide and resuspended in 2 ml of ice-cold 10

**Figure 1.** Late pathway of ergosterol biosynthesis in yeast with emphasis on the steps catalyzed by Erg6p (C-24 sterol methyltransferase) and Erg2p (C-8 sterol isomerase).



mM sodium azide. The final  $A_{600}$  was then adjusted to 0.5 with ice-cold 10 mM sodium azide. Two 0.5-ml aliquots of each sample were transferred to fresh microfuge tubes. To one aliquot of cells, 50  $\mu$ l of distilled water were added, and the cells were left on ice (whole cells). To the other aliquot of cells, 50  $\mu$ l of 10% Triton X-100 were added. Cells of this aliquot were permeabilized by freezing in liquid nitrogen and thawing at room temperature (lysates) and placed on ice. Aliquots of whole cells and lysates were assayed for invertase enzyme activity using the method of Goldstein and Lampen (1975). Ten-microliter samples were added in duplicate to 25  $\mu$ l of 0.2 M sodium acetate, pH 4.9, and 12.5  $\mu$ l of 0.5 M sucrose on ice. For the standard curve, known amounts of glucose (0, 12.5, 25, 50, 75, and 112.5 nmol) were used in place of the sample and sucrose. The tubes were incubated at 37°C for 10 min and then placed on ice. The reaction was terminated, and the invertase was inactivated by addition of 50  $\mu$ l of 100 mM potassium phosphate buffer, pH 7, and heating to 90°C for 3 min followed by chilling on ice. After addition of 500  $\mu$ l of solution C (50  $\mu$ g/ml glucose oxidase [*Aspergillus niger*; Fluka], 10  $\mu$ g/ml horseradish peroxidase [Fluka], 10 mM potassium phosphate buffer, pH 7, 300  $\mu$ g/ml *o*-dianisidine [Sigma, St. Louis, MO], and 38% wt/vol glycerol), the samples were incubated at 30°C for 20 min. The assay was terminated, and the color was developed by addition of 750  $\mu$ l of 6 M HCl. Absorbance at 540 nm was determined spectrophotometrically.

The readings for the duplicate samples were averaged. The internal invertase activity was calculated from the difference between the total invertase activity (from lysates) and the surface invertase activity (from whole cells) at each time point. The  $A_{540}$  values for the duplicate glucose standards were also averaged and plotted to give a glucose standard curve. The  $A_{540}$  values for the total, external, and internal invertase in the cell samples were then converted into nanomoles of glucose formed using the calculated slope of the glucose standard curve as a conversion factor (usually  $\sim 1 A_{540}$  unit represents 100 nmol of glucose). The internal and external invertase activity was then expressed as micromoles of glucose formed per  $A_{600}$  unit of cells per minute and plotted as a function of time after invertase induction.

### Sterol Analysis

Cells were grown to early logarithmic phase ( $0.7\text{--}1.0 \times 10^7$  cells/ml) in YPUATD medium at 24°C. Total sterols were extracted from whole cells based on a procedure by Folch *et al.* (1957). Alkaline hydrolysis was carried out as described by Lewis *et al.* (1987). Briefly,  $\sim 1 \times 10^9$  cells were harvested by centrifugation, resuspended in prewarmed YPUATD medium, and incubated for 30 min at 24 or 37°C. Harvested cells were then washed twice in distilled water to remove traces of the YPUATD medium. Cells were resuspended in a lysis solution comprising 1.5 ml of methanol (100%), 1 ml of 0.5% Pyrogallol (wt/vol in 100% methanol), and 1 ml of 60% KOH and heated for 2 h at 85°C. Total sterols were then extracted (three times) with 3 ml of petroleum ether. Upper phases were combined, dried under constant nitrogen gas, and stored at  $-20^\circ\text{C}$ . Before subjection to gas-liquid chromatography (GLC) and GLC-mass spectrometry (GLC-MS) analysis, dried sterols were resuspended in 0.5 ml of cyclohexane (Fluka). Individual sterols were analyzed by GLC (HP 5 column) and GLC-MS (HP 5-MS column; Hewlett Packard) as described by van den Hazel *et al.* (1999). Relative retention times of sterols were in agreement with previous

reports (Patterson, 1971; Xu *et al.*, 1988; Nes *et al.*, 1989). The abundance estimate of each sterol was based on two independent experiments analyzed in duplicate by GLC.

### Sterol Structure Drawings

The sterol structures shown in Figures 1 and 8 were drawn using the ChemSketch 3.5 software purchased from Advanced Chemistry Development (Toronto, Ontario, Canada).

## RESULTS

### *END11 Is Allelic to ERG2, the Gene Encoding C-8 Sterol Isomerase*

The wild-type *END11* gene was isolated by complementation cloning based on the growth defect associated with *end11-1*. For this purpose, the *end11-1* mutant strain was transformed with a yeast genomic library carried on a centromeric vector. Sequence analysis of a complementing plasmid, pEND11.2, revealed that the plasmid carried the *ERG2* gene (Arthington *et al.*, 1991). Transformation of *end11-1* cells with the *ERG2*-containing plasmid restored cell growth to wild-type rates (our unpublished results). In addition, mutant cells transformed with this plasmid were able to accumulate the fluorescent dye LY in vacuoles (our unpublished results), indicating that the plasmid-borne *ERG2* gene was able to complement the fluid phase endocytic defect of *end11-1* (Munn and Riezman, 1994). An integrative mapping strategy further demonstrated that the *ERG2* gene and the *end11-1* mutation are tightly linked (see MATERIALS AND METHODS).

The *ERG2* gene encodes C-8 sterol isomerase, an enzyme that functions in a late step of the ergosterol biosynthetic pathway (Arthington *et al.*, 1991). Absence of ergosterol is known to confer nystatin-resistant growth. Nystatin is an antifungal drug that interacts selectively with membrane ergosterol but not with sterols different from ergosterol (Lees *et al.*, 1995). As reported for *erg2* mutant strains (Arthington *et al.*, 1991), *end11-1* is able to grow on nystatin. Taken together, these results confirm that *END11* is allelic to *ERG2*.

### *erg2 $\Delta$ , erg6 $\Delta$ , and erg2 $\Delta$ erg6 $\Delta$ Mutants Exhibit Defects in the Internalization Step of Endocytosis*

The identification of *END11* as *ERG2* was the first indication that ergosterol is required for endocytosis in yeast. To examine the *in vivo* requirement for ergosterol in endocytosis in more detail, we made use of *erg $\Delta$*  mutants affected in the late ergosterol biosynthetic pathway. Each of these mutants accumulates a distinct set of sterols with structural differences specific to the ergosterol molecule (Lees *et al.*, 1995; Parks *et al.*, 1995). For this purpose, the *ERG2* and *ERG6*

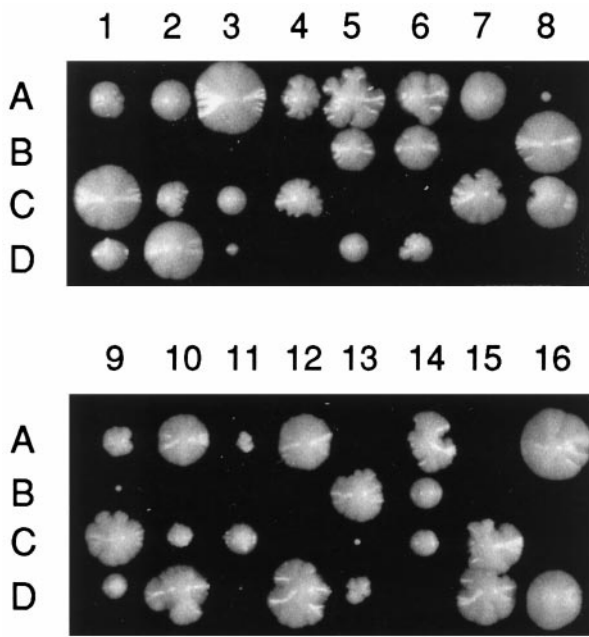


**Figure 2.** Dissection plate of the diploid strain *erg2Δ/ERG2 erg6Δ/ERG6* (RH3610). Spores (A–D) from each tetrad (1–14) were allowed to germinate and grow on YPUATD at 24°C. In viable spores were those predicted to have the genotype *erg2Δerg6Δ*. A few spores of this genotype were viable (8A and 9B) but grew extremely slowly.

genes were disrupted by integration replacements (see MATERIALS AND METHODS). Erg2p, the C-8 sterol isomerase, is involved in changes of the B ring desaturation, whereas Erg6p, the C-24 sterol methyltransferase, modifies the sidechain of the sterol molecule (Figure 1). An *erg2Δerg6Δ* double mutant strain lacks both Erg2p and Erg6p activities and has been reported to accumulate mainly zymosterol (Bard *et al.*, 1977; Figure 1; see below).

Consistent with previous reports, deletions of the *ERG2* and *ERG6* genes did not cause lethality (Gaber *et al.*, 1989; Arthington *et al.*, 1991; Hardwick and Pelham, 1994; Welihinda *et al.*, 1994). The *erg2Δ* strains showed a slow-growth phenotype at 24 and 37°C similar to that observed for *end11-1* (our unpublished results). The *erg6Δ* strain grew at wild-type rates at 24°C, but its growth was reduced at 37°C (our unpublished results). Double mutant strains (*erg2Δerg6Δ*) were isolated after mating *erg2Δ* and *erg6Δ* haploid strains, sporulation, and dissection of the diploid. Most double mutant spores were inviable, but occasionally they gave rise to extremely slow-growing colonies (Figure 2; see spores 8A and 9B). Spores that were wild type, *erg2Δ*, or *erg6Δ* were nearly all viable and grew relatively well. When surviving double mutant haploids were crossed back to a wild-type strain, each resulting diploid gave rise to wild-type, *erg2Δ*, *erg6Δ*, as well as *erg2Δerg6Δ* mutant spores. In each case, the double mutant spores were mostly inviable, demonstrating that the surviving double mutant haploids from the first cross used as one parent did not possess an extragenic suppressor mutation. Two of these slow-growing *erg2Δerg6Δ* double mutants were retained for further analysis.

Fluid phase and receptor-mediated endocytosis were examined in *erg2Δ*, *erg6Δ*, and *erg2Δerg6Δ* mutant strains and compared with endocytosis in the wild-type strain. In assays for fluid phase endocytosis, yeast cells were incubated with the fluorescent dye LY at 24°C for 1 h and observed by fluorescence microscopy. As shown for the wild-type strain (Figure 3A; Riezman, 1985), endocytic uptake of the dye resulted in LY accumulation in yeast vacuoles that were visible as indentations in the Nomarski image (Figure 3B). The *erg6Δ* cells accumulated LY in vacuoles to similar levels as wild-type cells (Figure 3E), indicating no apparent block in fluid phase endocytosis. In contrast, *erg2Δ* and *erg2Δerg6Δ* cells were clearly defective in fluid phase endocytosis, because little or no fluorescent dye was present in vacuoles (Figure 3, C and G, respectively). The block in fluid phase endocytosis of *erg2Δ* cells was consistent with the results obtained for *end11-1* (Munn and Riezman, 1994). It should be noted that some *erg2Δ* and *erg2Δerg6Δ* cells did not contain a recognizable vacuole in Nomarski images; however, those containing an obvious vacuole did not accumulate the fluorescent dye (Figure 3, D and H). The strong cytoplasmic staining in some *erg2Δerg6Δ* cells (Figure 3G) may be due to loss of viability that was also observed in subsequent experiments. We also observed that many *erg2Δerg6Δ* cells exhibited stronger cytoplasmic staining than wild-type or *ergΔ* single mutant cells indicating that the *ergΔ* double mutant cells may be more permeable to the dye.

To assay the first step of receptor-mediated endocytosis, radiolabeled  $\alpha$ -factor was added to *ergΔ* mutant and wild-type cells that had been preincubated for 15 min at 24 or 37°C. Internalization of the  $\alpha$ -factor receptor–ligand complex at the given temperature was then examined by determining the percentage of internal radiolabeled  $\alpha$ -factor at specific time points. Consistent with previous reports (Munn and Riezman, 1994; Munn *et al.*, 1995), internalization of  $\alpha$ -factor in wild-type cells was similar at 24 and 37°C (Figure 4). The *ergΔ* single and double mutant cells exhibited reduced internalization at 24°C, but the defect was stronger at 37 than at 24°C (Figure 4). While wild-type cells internalized most of the  $\alpha$ -factor within 30 min (Figure 4A), *erg2Δ* cells exhibited a defect in  $\alpha$ -factor internalization similar to that reported previously for *end11-1* cells (Figure 4A; Munn and Riezman, 1994). These results indicate that cells lacking the C-8 sterol isomerase activity have a defect in the internalization step, the first step of endocytosis. Internalization was also reduced in *erg6Δ* cells (Figure 4B), but to a lesser extent than in *erg2Δ* cells (Figure 4A). In contrast to LY uptake,  $\alpha$ -factor internalization is a quantitative assay (Dulic *et al.*, 1991), and it is possible that a mild endocytic defect in *erg6Δ* cells was not apparent in the LY accumulation experiment (Figure 3). In *erg2Δerg6Δ* double mutant cells,  $\alpha$ -factor internalization was completely abolished at 37°C (Figure 4C). Thus at 37°C, cells lacking both C-24 sterol methyltransferase and C-8 sterol isomerase activities show endocytic defects as severe as those observed in the tightest *end* mutants blocked in the internalization step of endocytosis, such as *end3-1*, *end4-1* (Raths *et al.*, 1993), and *act1-1* (Kübler and Riezman, 1993).

After internalization of the  $\alpha$ -factor receptor–ligand complex, the complex moves through early and late endosomal compartments to the vacuole where it is degraded. To determine whether later steps in the endocytic pathway were



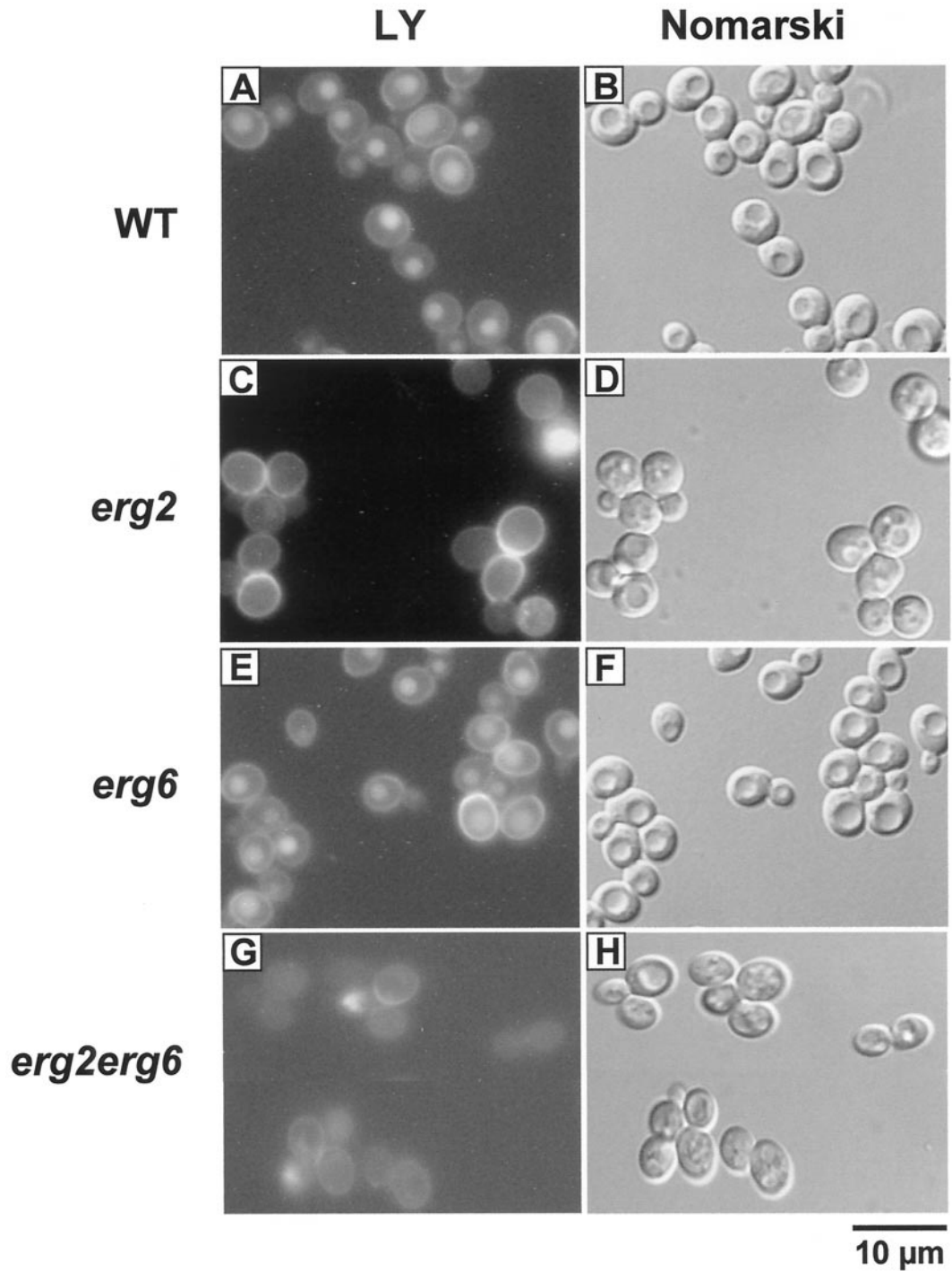


**Figure 3.** Analysis of fluid phase endocytosis in *ergΔ* mutant cells. Wild-type (RH448; A and B), *erg2Δ* (RH2897; C and D), *erg6Δ* (RH3622; E and F) and *erg2Δerg6Δ* (RH3616; G and H) cells were incubated with LY at 24°C. To visualize the localization of LY, cells were viewed by FITC-fluorescence optics (A, C, E, and G). The same fields of cells were examined by Nomarski optics to visualize the vacuoles (which are apparent as indentations in the cell profiles; B, D, F, and H). Bar, 10 μm.

also affected in *ergΔ* mutant cells,  $\alpha$ -factor degradation assays were performed at 37°C (Dulic *et al.*, 1991). In wild-type cells, most of the  $\alpha$ -factor was internalized within 30 min (Figure 5A; pH1 resistant) and then delivered to the vacuole as evident by the accumulation of degraded  $\alpha$ -factor at later timepoints (Figure 5A, d). Consistent with a defect in the internalization step, some intact  $\alpha$ -factor remained at the cell

surface of *erg2Δ* and *erg6Δ* mutant cells even after 90 min (Figure 5, B and C, i; pH 6 resistant). The *erg2Δ* and *erg6Δ* mutant cells did not, however, exhibit strong defects at a postinternalization step, because degraded  $\alpha$ -factor was present at later time points (Figure 5, B and C, d). We were unable to perform the degradation assay on the *erg2Δerg6Δ* double mutant because insufficient amounts of  $\alpha$ -factor were

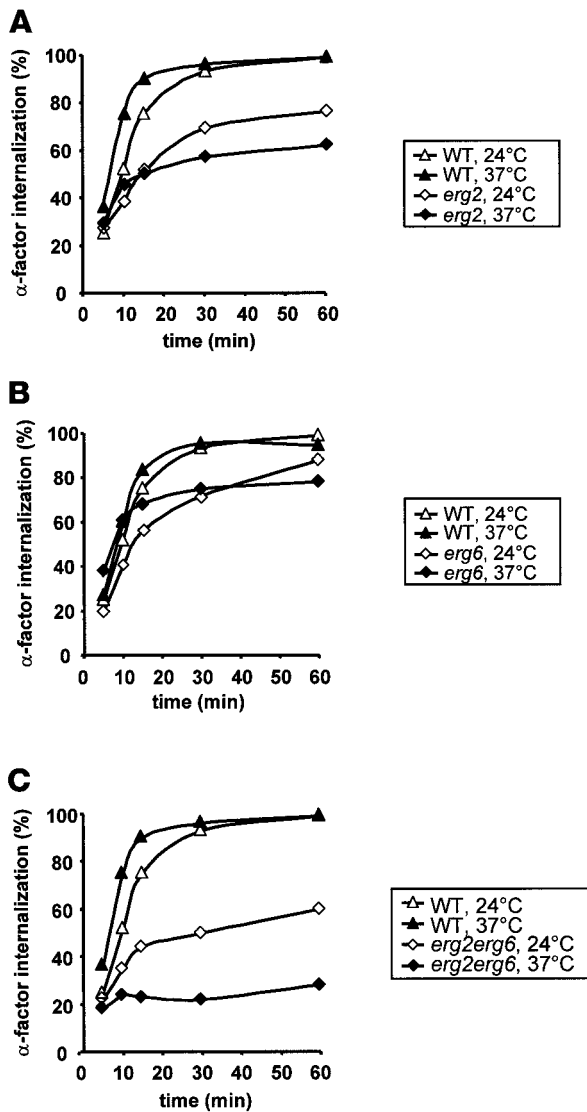


**Figure 4.** Analysis of the internalization step of receptor-mediated endocytosis in *ergΔ* mutant cells. Internalization assays were performed at 24°C (open symbols) and 37°C (closed symbols) on *erg2Δ* (RH2897; A), *erg6Δ* (RH3622; B), and *erg2Δerg6Δ* (RH3616; C) mutant and wild-type cells (RH1800; A–C). Internalization of radiolabeled  $\alpha$ -factor was expressed as a percentage by dividing internalized counts by the total cell-associated counts for each time point.

internalized in this *ergΔ* mutant because of the severity of the defect. Based on these endocytic assays, we conclude that specific sterols are required for the internalization step of endocytosis in yeast.

***erg2Δ*, *erg6Δ*, and *erg2Δerg6Δ* Mutations Do Not Affect Maturation of CPY or Secretion of Invertase to the Plasma Membrane**

Ergosterol is predominately present in the plasma membrane, but it is also found in significant amounts in secretory

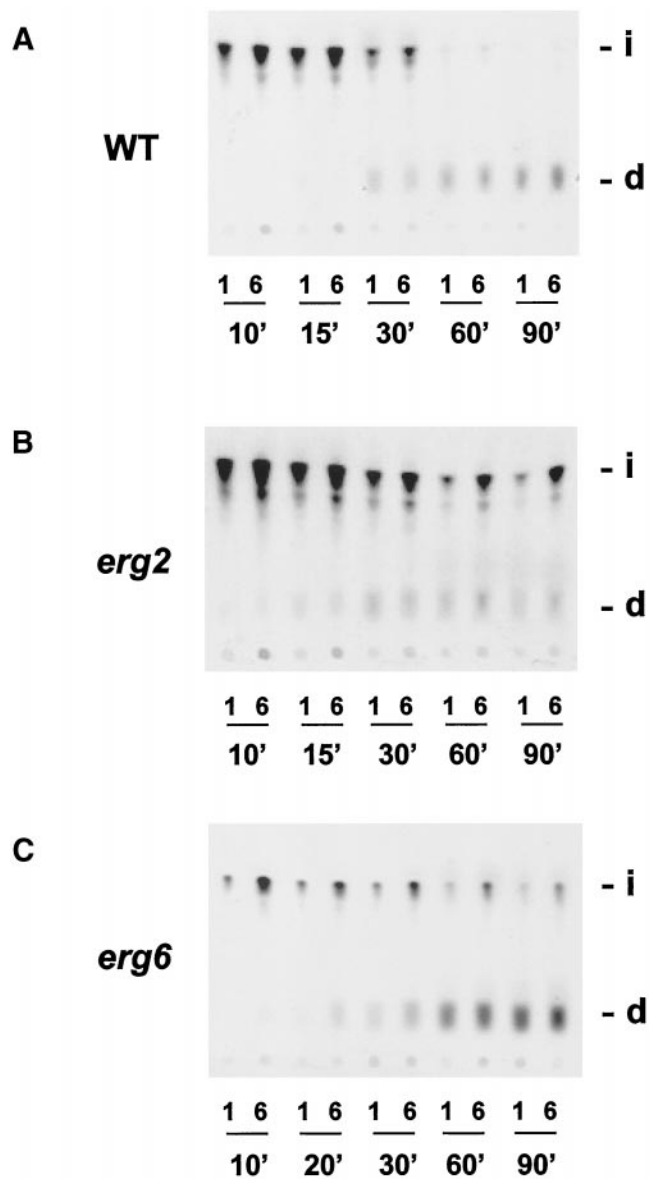
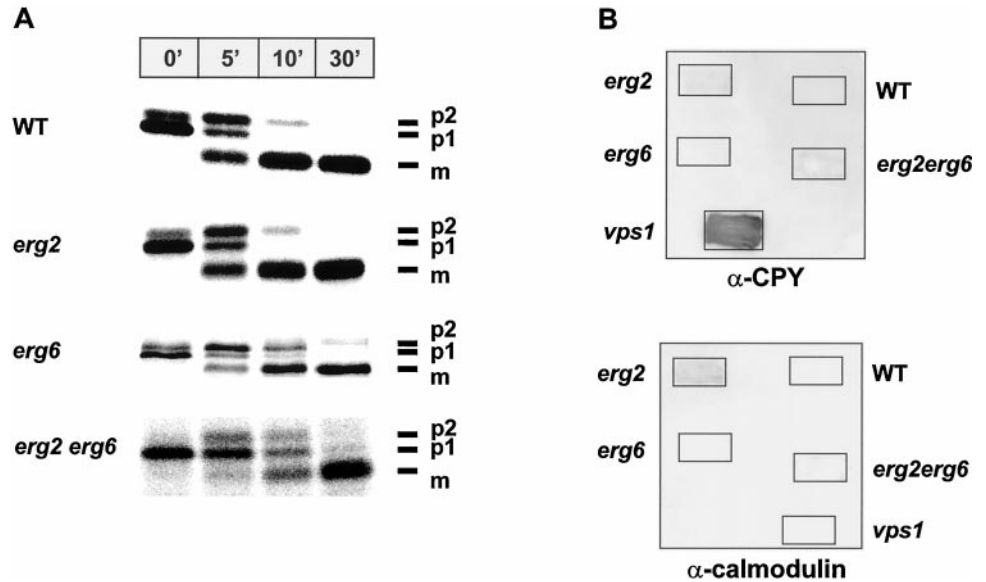


**Figure 5.** Analysis of  $\alpha$ -factor degradation in *ergΔ* mutant cells.  $\alpha$ -Factor degradation assays were performed at 37°C on wild-type (RH1800; A), *erg2Δ* (RH2897; B), and *erg6Δ* (RH3622; C) cells. At times indicated, samples were taken and diluted in pH1 buffer (1; internalized counts) or pH6 buffer (6; total cell-associated counts). Degradation of  $\alpha$ -factor was assessed by extracting cell-associated radioactivity and separating degraded  $\alpha$ -factor (d; indicating delivery to the vacuole) from intact  $\alpha$ -factor (i) on TLC plates. d, degraded  $\alpha$ -factor; i, intact  $\alpha$ -factor; n', time in minutes.

vesicles (Zinser *et al.*, 1993). We therefore investigated whether the sterol requirement is specific for the formation of endocytic vesicles or whether vesicular trafficking through the secretory pathway also requires ergosterol. By monitoring maturation of the newly synthesized CPY precursor, we followed the vesicular transport of CPY from the endoplasmic reticulum (ER) to the Golgi and then to the



**Figure 6.** Sorting of newly synthesized CPY to the vacuole in *ergΔ* mutant cells. (A) Maturation of newly synthesized CPY in wild-type (RH1800), *erg2Δ* (RH2897), *erg6Δ* (RH3622), and *erg2Δerg6Δ* (RH3617) cells. Cells were grown at 24°C, shifted to 37°C for 15 min, and then pulse labeled at 37°C for 5 min with [<sup>35</sup>S]methionine and [<sup>35</sup>S]cysteine followed by a chase with nonradioactive sulfate, methionine, and cysteine at 37°C. CPY was immunoprecipitated from samples taken at specified time points of chase (minutes). The immunoprecipitates were resolved on 7.5% SDS-polyacrylamide gels and visualized on a PhosphorImager. p1, core glycosylated precursor form of CPY; p2, fully glycosylated precursor form of CPY; m, proteolytically processed, mature CPY; n', time in minutes. (B) Sorting of CPY to the vacuole in wild-type (RH1800), *erg2Δ* (RH2897), *erg6Δ* (RH3622), *erg2Δerg6Δ* (RH3617), and *vps1Δ* (RH2180) cells. Cells were grown as patches on YPUATD solid medium in contact with nitrocellulose filters at 24°C. Washed filters were probed with either rabbit polyclonal antibodies against CPY ( $\alpha$ -CPY) or calmodulin ( $\alpha$ -calmodulin) followed by goat anti-rabbit immunoglobulin G coupled to horseradish peroxidase. Any CPY secreted or any calmodulin released from the cells was visualized by enhanced chemiluminescence.



vacuole in the *ergΔ* mutant and wild-type strains (Figure 6A). It has been previously shown for wild-type cells (Stevens *et al.*, 1982; Klionsky *et al.*, 1990) that upon translocation into the ER, CPY is core glycosylated to generate a form with an apparent molecular mass of 67 kDa (p1). This precursor protein is further glycosylated to the 69-kDa form (p2) in an early Golgi compartment, and upon arrival in the vacuole, the p2 form is cleaved to the mature and active CPY of 61 kDa (m). Pulse-chase labeling experiments followed by immunoprecipitation of CPY showed that CPY matures in *ergΔ* single and double mutant strains with kinetics similar to those observed in the wild-type strain (Figure 6A). The p1 form of CPY seems to be converted to the p2 form slightly more slowly than in wild-type cells, but this defect is mild when compared with the defects in growth rate and endocytosis exhibited in the *erg2Δerg6Δ* mutant cells by the double mutant. These results are in agreement with previous reports that *end11-1* (Munn and Riezman, 1994) and *erg6Δ* (Hardwick and Pelham, 1994; isolated as *sed6*) do not have a defect in CPY maturation.

Some mutants defective in transport of CPY to the vacuole (vacuole protein-sorting [*vps*] mutants) do not exhibit defects in maturation of intracellular CPY but still missort significant amounts of p2 CPY to the cell surface (Robinson *et al.*, 1988). Therefore, we also assayed secretion of CPY in the *ergΔ* mutants by colony immunoblotting using antibodies against CPY. As expected, a *vps1* control strain showed high levels of CPY secretion (Figure 6B,  $\alpha$ -CPY; Robinson *et al.*, 1988). However, none of the *ergΔ* mutants or the wild-type strain showed significant secretion of CPY into the medium (Figure 6B,  $\alpha$ -CPY). The release of trace amounts of CPY antigen in *erg2Δ* and *erg2Δerg6Δ* mutant strains were likely caused by occasional cell lysis, because these strains

also released low levels of calmodulin, a cytoplasmic protein (Figure 6B,  $\alpha$ -calmodulin).

To determine whether *ergΔ* mutations affect protein secretion to the plasma membrane, we analyzed secretion of invertase. In wild-type cells, invertase is secreted into the periplasm between the plasma membrane and the cell wall. Initial attempts to measure invertase secretion by pulse-chase radiolabeling of spheroplasts were unsuccessful, because *ergΔ* mutant strains had a tendency to lyse upon removal of the cell wall, even in the presence of osmotic support. As an alternative approach, internal and external invertase activities were measured using enzyme latency assays that do not require the removal of the cell wall (Rothman *et al.*, 1986). In these assays, it is possible to differentiate between internal and external invertase activities, because the substrate (sucrose) can diffuse easily across the cell wall but not the plasma membrane. Internal invertase activity was then calculated from the difference between external invertase activity in whole cells and total invertase activity in cell lysates at each time point. Even though invertase activity was induced to different levels within each strain, *erg2Δ* [Figure 7B, (e)], *erg6Δ* [Figure 7C, (e)], and *erg2Δerg6Δ* [Figure 7D(e)] mutant strains secreted invertase with wild-type kinetics [Figure 7A, WT (e)]. Similar amounts of internal invertase were detected in wild-type cells and any of the *ergΔ* mutant cells. In contrast, a *sec18* mutant strain (defective in ER-to-Golgi transport of secreted proteins) did not secrete invertase into the periplasm but accumulated invertase internally (Figure 7A; Novick *et al.*, 1981). Taken together, these data indicate that sterols present in *erg2Δ*, *erg6Δ*, and *erg2Δerg6Δ* mutant strains are capable of supporting vesicle formation and fusion throughout the secretory pathway, including vesicle fusion to the plasma

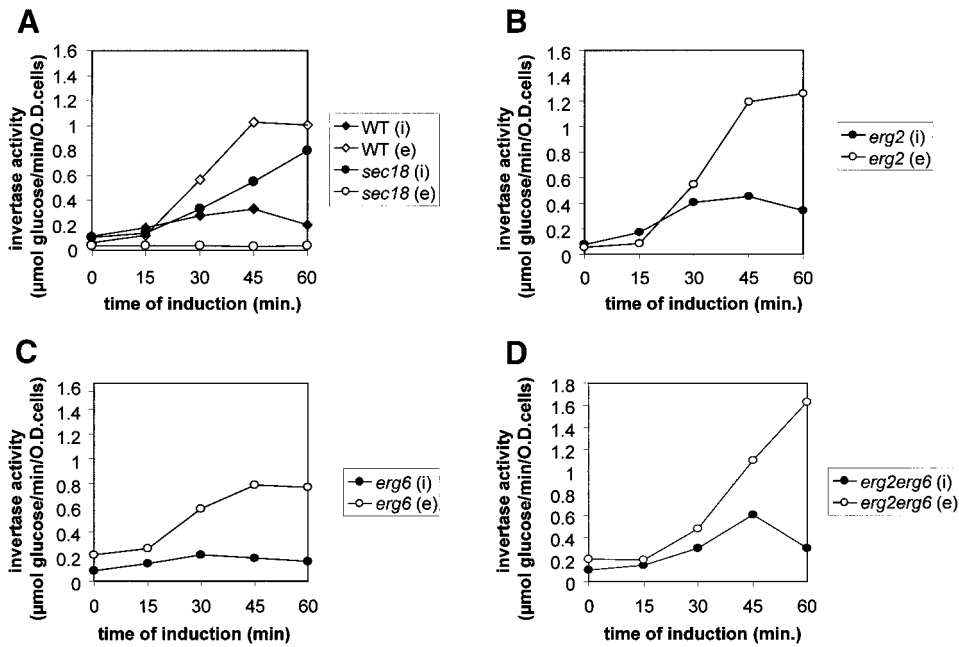


**Figure 7.** Secretion of invertase in *ergΔ* mutant cells. Invertase activities were assayed in wild-type (RH1800; A), *sec18* (RH1737; A), *erg2Δ* (RH2897; B), *erg6Δ* (RH3622; C), and *erg2Δerg6Δ* (RH3617; D) cells. Internal invertase activity (i) was calculated from the difference between the total invertase activity (cell lysate) and the surface invertase activity (whole cell; e) at each time point. Internal and external invertase activities were expressed as micromoles of glucose formed per  $A_{600}$  units of cells per min and plotted as a function of time after invertase induction. Open symbols, extracellular invertase activities (e); closed symbols, intracellular invertase activities (i); O.D., optical density.

membrane, but do not allow the formation of endocytic vesicles at the plasma membrane.

#### Determining the Sterol Composition of *ergΔ* Single and Double Mutants

The sterol composition of *erg2Δ*, *erg6Δ*, and *erg2Δerg6Δ* mutant strains has been described previously for cells in stationary growth phase (Bard *et al.*, 1977; Gaber *et al.*, 1989; Arthington *et al.*, 1991). It appears, however, that the sterol composition can vary depending on growth conditions and the stage of cellular growth (Leber *et al.*, 1995). All of our previously described experiments were performed on cells in early log phase, a growth phase at which the exact sterol composition of the *ergΔ* mutants and the wild-type strain is unknown. To correlate the internalization defects with the sterol compositions of the *ergΔ* mutants, it was therefore necessary to determine the sterol composition of each *ergΔ* mutant and wild-type strain under the same growth conditions used for the experiments described above. As mentioned previously, *ergΔ* single and double mutant cells exhibited defects in  $\alpha$ -factor internalization after incubation at 24°C; however, these defects were more severe after incubation at 37°C (Figure 4). To investigate whether these effects on internalization were due to changes in the overall sterol composition, total sterols were isolated from whole yeast cells that were grown to early log phase at 24°C and then incubated for 30 min at either 24 or 37°C. Individual sterols were separated by GLC and GLC-MS (van den Hazel *et al.*, 1999). Based on the retention time and the mass spectrum of each sterol, we were able to identify nearly all sterols present in the *ergΔ* mutant and wild-type strains (Table 2). In addition, we calculated the abundance of each sterol within a given strain (Table 2). Preincubation of cells at 24 or 37°C did not lead to significant changes in the overall sterol composition in any of the analyzed strains (Table 2; our unpub-

lished results). This result indicates that the more severe internalization defect observed in the *ergΔ* mutant cells when incubated at 37°C is not due to an altered sterol composition.

Many of the ergosterol biosynthetic enzymes are able to act on a range of sterol substrates, indicating that the ergosterol biosynthetic pathway is not strictly linear (reviewed in Lees *et al.*, 1995; Parks and Casey, 1995). An *erg* mutant can therefore accumulate a variety of sterol analogues rather than only one ergosterol precursor. Overall, the sterol compositions of the *ergΔ* mutant and wild-type strains were in agreement with previous reports (Bard *et al.*, 1977; Gaber *et al.*, 1989; Arthington *et al.*, 1991). The predominant sterol in the wild-type strain was ergosterol (77%; Table 2 and Figure 8). As expected, none of the *ergΔ* strains accumulated any detectable amount of ergosterol. These results are in agreement with previous studies, which reported that under aerobic growth conditions yeast cells are unable to internalize sterols from the extracellular medium (Trocha and Sprinson, 1976; Keesler *et al.*, 1992). Consistent with the absence of the C-8 sterol isomerase activity, the *erg2Δ* mutant strain accumulated sterols that lack a C-7,8 double bond. The major sterols in this mutant were ergosta-8-enol (35.4%), fecosterol (33.3%), and ergosta-5,8,22-trienol (12.7%; Table 2 and Figure 8). Consistent with a lack of the C-24 sterol methyltransferase activity, all sterols in the *erg6Δ* mutant strain were missing the C-24 methylation, and zymosterol (39.4%) and cholesta-5,7,24-trienol (32.2%) were the most abundant sterols (Table 2 and Figure 8). The *erg2Δerg6Δ* double mutant strain accumulated nearly exclusively zymosterol (85.6%), an intermediate in the late part of the ergosterol biosynthetic pathway. Based on these sterol data, we were able to correlate the endocytic phenotypes of the *ergΔ* mutant and wild-type strains to their sterol composition and abundance of the major sterols.

**Table 2.** Analysis of the sterol composition and the relative abundance of sterols within wild-type (RH448), *erg2* (RH2897), *erg6* (RH3622), and *erg2erg6* (RH3616) cells

Sterol	% sterol	Mass
WT		
Zymosterol	6.9	384
Ergosterol	77	396
Fecosterol	3	398
A	5.1	398
Episterol	3.2	398
Lanosterol	3.8	426
<i>erg2</i>		
Squalene	1.4	410
Zymosterol	5	384
Ergosta-5,8,22-trienol	12.7	396
Ergosta-7,22-dienol	4.3	398
Fecosterol	33.2	398
Ergosta-8-enol	35.4	400
B	1.6	396
4-m-Cholesta-8,24-dienol	2.5	398
Lanosterol	2.9	426
4,4-dm-Cholesta-8,24-dienol	1.1	412
<i>erg6</i>		
Squalene	1.3	410
Cholesta-5,8,24-trienol	2.8	382
Zymosterol	39.4	384
Cholesta-5,7,24-trienol	32.2	382
Cholesta-7,24-dienol	7.3	384
Cholesta-5,7,22,24-tetraenol	7.9	380
C	2.7	398
Lanosterol	3.1	426
4,4-dm-Cholesta-8,24-dienol	2.3	412
<i>erg2erg6</i>		
Squalene	2.7	410
Zymosterol	85.6	384
D	3.7	382
E	1.5	398
Lanosterol	3.3	426
4,4-dm-Cholesta-8,24-dienol	2.1	412

After growth at 24°C to midlog phase, cells were incubated for 30 min at 37°C. Total sterols were isolated from whole cells and subjected to GLC and GLC-MS to identify individual sterols and to determine the abundance of each sterol within a strain. WT, wild type; 4,4-dm-cholesta-8,24-dienol, 4,4-dimethyl-cholesta-8,24-dienol; 4-m-cholesta-8,24-dienol, 4-methyl-cholesta-8,24-dienol; A–E, identification of sterols uncertain.

## DISCUSSION

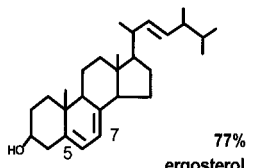
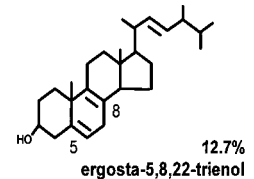
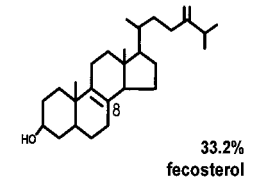
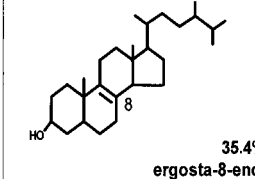
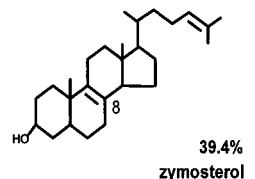
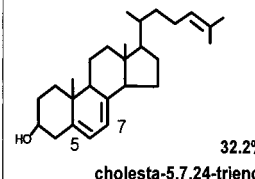
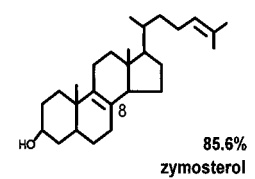
In the present study, we identified a novel function of sterols in yeast, that is, facilitating endocytosis. The first evidence for this endocytic function came from the identification of *END11*, whose gene product is required for the internalization step of endocytosis (Munn and Riezman, 1994), as *ERG2*. This gene encodes the C-8 sterol isomerase, which functions in a late step of ergosterol biosynthesis (Arthington *et al.*, 1991; Figure 1). Cells with a deleted *ERG2* gene show internalization defects similar to those observed for *end11-1*. These endocytic defects are due to the altered sterol composition rather than to a novel function of Erg2p in endocytosis. An internalization defect, although a weaker one, was also observed in an *erg6*Δ strain that lacks the C-24

sterol methyltransferase activity of Erg6p. This transferase has no structural nor functional similarities to Erg2p, an isomerase. Furthermore, studies using animal cells indicate that depletion of cholesterol leads to internalization defects of certain proteins (Chang *et al.*, 1992; Cerneus *et al.*, 1993; Deckert *et al.*, 1996; Orlandi and Fishman, 1998; Rodal *et al.*, 1999).

In animal cells, the sterol requirement has been mainly investigated by using drugs such as filipin, nystatin, and β-cyclodextrin that bind and sequester cholesterol (Chang *et al.*, 1992; Cerneus *et al.*, 1993; Deckert *et al.*, 1996; Orlandi and Fishman, 1998; Rodal *et al.*, 1999; Subtil *et al.*, 1999). In contrast, the yeast *erg*Δ mutants allowed us to examine the *in vivo* requirement for sterols without the use of drugs and sterol depletion. Moreover, we were able to assess the importance of particular structural features of the ergosterol molecule for the internalization step, because the *erg*Δ mutants accumulate sterols that are different from ergosterol. After the identification of End11p as Erg2p, the C-8 sterol isomerase involved in the B ring modification of ergosterol, we chose to examine endocytosis in *erg* mutants reported to accumulate sterols with changes in the side chain modification and in both B ring desaturation and side chain modification. The obvious choice was to construct an *erg6*Δ strain lacking the C-24 sterol methyltransferase activity (Gaber *et al.*, 1989) and an *erg2*Δ*erg6*Δ strain lacking both C-8 sterol isomerase and C-24 sterol methyltransferase activities. Interestingly, internalization of the α-factor receptor–ligand complex was inhibited to different extents in each *erg*Δ strain. By taking the sterol composition and sterol abundance of each *erg*Δ mutant and the wild type into account, we were able to correlate defects in internalization to the altered sterol composition. More importantly, it enabled us to correlate the internalization defect to a specific portion of the ergosterol molecule, namely to the B ring and its desaturation state.

Ergosterol, the main sterol in the wild-type strain, can fully support the internalization step of endocytosis at 24 and 37°C. In contrast, *erg2*Δ*erg6*Δ cells with zymosterol as their predominant sterol showed the strongest defect in internalization. Zymosterol has a double bond at C-8,9 but lacks both of the double bonds (C-5,6 and C-7,8) present in the B ring of ergosterol (Table 2 and Figure 8). In addition, zymosterol does not have the C-24 methylation present in ergosterol. The C-24 methylation did not appear to play a major role in the internalization step, because all sterols present in the *erg6*Δ strains lack this modification (Table 2 and Figure 8), and the *erg6*Δ strain did not exhibit a strong internalization defect. It seems more likely that the state of the B ring desaturation is mainly responsible for the endocytic defects. The rate of internalization correlated well with the abundance of sterols with two double bonds at C-5,6 and C-7,8 or at C-5,6 and C-8,9, and it correlated inversely with the abundance of sterols with a single desaturation at C-8,9. The *erg2*Δ*erg6*Δ double mutant cells had the highest amount of sterols with a single C-8,9 desaturation in the B ring (>85%) and also showed the strongest internalization defect. In addition, >75% of sterols in *erg2*Δ cells had a single C-8,9 desaturation in the B ring. Its internalization defect was less severe than that observed in the *erg2*Δ*erg6*Δ double mutant strain, but it was more severe than that in *erg6*Δ cells. Even though the *erg2*Δ strain did not accumulate any C-7,8 sterols, it showed some internalization of α-factor. It is reasonable to



WT			
<i>erg2</i>			
<i>erg6</i>			
<i>erg2erg6</i>			

**Figure 8.** Chemical structures of the most abundant sterols (>10%) present in wild-type (RH448), *erg2* $\Delta$  (RH2897), *erg6* $\Delta$  (RH3622), and *erg2* $\Delta$ *erg6* $\Delta$  (RH3616) cells. The abundance of each sterol within a strain is given as a percentage of total sterol.

assume that the relatively low amounts of ergosta-5,8,24-trienol (12.7%), a sterol containing two desaturations in the B ring at positions C-5,6 and C-8,9, is responsible for this  $\alpha$ -factor internalization. These results indicate that even though a single desaturation in the B ring at C-8,9 is not able to support internalization, an additional C-5,6 desaturation (leading to a B ring desaturation at both C-5,6 and C-8,9) allows internalization of  $\alpha$ -factor at 37°C. In addition to the C-8,9 sterols (~40%), the *erg6* $\Delta$  strain accumulated >30% of cholesta-5,7,24-trienol, a sterol containing the exact B ring desaturation (C-5,6 and C-7,8) present in ergosterol. It is likely that cholesta-5,7,24-trienol is able to support endocytosis, but there is simply not enough of this sterol present in the *erg6* $\Delta$  strain to support endocytosis with wild-type kinetics.

Taking these arguments together, we conclude that the state of the B ring desaturation is critical for the internalization step of endocytosis. While a single desaturation at C-8,9 was not sufficient to support internalization of  $\alpha$ -factor at 37°C, the presence of two double bonds in the B ring, either a combination of C-5,6 and C-7,8 or C-5,6 and C-8,9, allowed internalization to occur at this temperature. The methylation at C-24 in the side chain did not appear to be required for the internalization step of endocytosis, because its absence did not have a strong effect on  $\alpha$ -factor uptake. At this point, the exact location of each sterol remains unknown in the *erg* $\Delta$  strains. It is reasonable to assume that the sterols with altered structural features were present in the plasma mem-

brane, because the majority of sterols are usually found in this membrane (Zinser *et al.*, 1993).

Clearly, sterols play an important role in the internalization step of endocytosis in yeast perhaps similar to the role of cholesterol in endocytosis in animal cells. Even though the overall structures of ergosterol and cholesterol are similar, three structural differences are evident in the B ring and the side chain. While cholesterol has only a single desaturation at C-5,6, ergosterol possesses two double bonds at C-5,6 and C-7,8. The side chain of ergosterol contains a desaturation at C-22,23 and a methyl group at C-24 that are both absent in cholesterol (for review, see Parks and Casey, 1995). Interestingly, the C-8 sterol isomerase (Erg2p) and the C-24 sterol methyltransferase (Erg6p) represent two of the enzyme activities that confer the structural differences between ergosterol and cholesterol. The absence of these two enzyme activities leads to the accumulation of zymosterol. As evident from the strong endocytic defect in the *erg2* $\Delta$ *erg6* $\Delta$  double mutant, zymosterol, containing a single C-8,9 desaturation in the B ring was unable to support internalization in yeast at 37°C. It seems likely that in general, ergosterol and cholesterol serve similar functions, but the structure of the sterols may be adjusted to suit the specific needs of the organism the sterols are present in. In a single-cell organism, such as yeast, ergosterol may satisfy a variety of functions, including some that may not be critical in multicellular organisms. In support of this hypothesis, other yeast lipids such as phospholipids and sphingolipids also

differ from the respective animal lipid in certain structural features (Daum *et al.*, 1998; Dickson, 1998).

Animal cells are able to obtain cholesterol by two ways: endogenously, by producing the sterol *de novo* in the ER, and exogenously, by internalizing cholesterol from the extracellular medium (Fielding and Fielding, 1997). In contrast, yeast has to rely on ergosterol produced endogenously, because under normal, aerobic growth conditions yeast is unable to take up sterols from the extracellular medium (Trocha and Sprinson, 1976; Keesler *et al.*, 1992). Consistent with these reports, we showed in the present studies that none of the *ergΔ* mutants was able to internalize ergosterol from the growth medium despite the presence of yeast extract, because no ergosterol was detected by GLC and GLC-MS analysis (Table 2). Furthermore, the  $\alpha$ -factor internalization defect in *erg2Δ* cells was similar whether the yeast cells were grown in synthetic medium lacking any lipids or in YPUATD containing yeast extract (our unpublished results). Although desirable, we were not able to perform ergosterol feedback experiments in these *ergΔ* mutants because of the sterol exclusion under growth conditions that are required for the endocytic assays.

Even though a role for sterols in endocytosis is evident, the question remains how sterols participate in the internalization step at the plasma membrane. Ergosterol may serve as a site for the interaction of the endocytic machinery with the plasma membrane. Similar to what has been observed for animal cells (for review, see Harder and Simons, 1997; Anderson, 1998; Brown and London, 1998), ergosterol may associate with sphingolipids to form lipid rafts that serve as platforms for the recruitment and subsequent internalization of specific proteins. Microdomains with some features in common with animal cell microdomains are present in yeast membranes (Kübler *et al.*, 1996). These microdomains have been proposed to function in signaling (Kübler *et al.*, 1996); however, neither their lipid composition nor their role in internalization has been determined. Little evidence exists for sterol-rich and -poor regions in yeast plasma membranes (Bottema *et al.*, 1983), nor is it known whether ergosterol can associate with sphingolipids to form lipid rafts (Leber *et al.*, 1997). In animal cells, depletion of cholesterol prevents clustering of glycosylphosphatidylinositol-anchored proteins into lipid rafts and, thus, blocks their subsequent internalization (Chang *et al.*, 1992; Rothberg *et al.*, 1990; Rothberg *et al.*, 1992). If the main role of ergosterol lies in the recruitment and clustering of proteins into sterol-rich domains, one might expect that only receptor-mediated but not fluid phase endocytosis would be defective in *ergΔ* mutants. This is not true for *erg2Δ* and *erg2Δerg6Δ*, because in addition to defects in  $\alpha$ -factor receptor internalization, these *ergΔ* mutants exhibit strong defects in fluid phase endocytosis. These results point toward a more general defect in endocytosis in *ergΔ* mutants.

Ergosterol may also provide a membrane environment required for the correct conformation of plasma membrane proteins that function in endocytosis. In support of this hypothesis, several plasma membrane proteins (Gaber *et al.*, 1989; Welihinda *et al.*, 1994) have been reported to function at reduced levels in *erg6Δ* mutants. We do not believe, however, that the endocytic defects observed in the *ergΔ* mutants are due to an inactivation of Ste2p, the  $\alpha$ -factor receptor. The  $\alpha$ -factor internalization and  $\alpha$ -factor degrada-

tion assays show that Ste2p is able to bind  $\alpha$ -factor, indicating that Ste2p is functional in plasma membranes with an altered sterol composition. In addition, the internalization defect in the *ergΔ* mutants is not specific for ligand-induced endocytosis of Ste2p, because we observed a severe block in fluid phase endocytosis in *erg2Δ* and *erg2Δerg6Δ* mutants.

Finally, ergosterol may play a crucial role in the physical formation of endocytic vesicles. Sterols are rigid and compact molecules consisting of a planar, nonpolar ring system and a single polar functional group, a hydroxyl group at C-3 (Brown, 1998). The orientation and conformation of sterols are important for their interaction with other lipids and influence membrane permeability and membrane fluidity (Brown, 1998; Daum *et al.*, 1998). As previously reported, alterations in the sterol composition change the fluidity of membranes, and the membrane fluidity decreases from wild type to *erg6Δ* to *erg2Δ* to *erg2Δerg6Δ*, with the double mutant showing the highest membrane rigidity (Lees *et al.*, 1979). Interestingly, an increase in membrane rigidity correlates well with the severity of the internalization defect for the *ergΔ* mutants reported in the present studies. It is interesting to note that even though the sterol compositions were similar at 24 and 37°C, each *ergΔ* mutant exhibited stronger internalization defects at higher temperatures. In particular,  $\alpha$ -factor internalization was completely blocked in the *erg2Δerg6Δ* mutant strain at 37°C. It is therefore possible that the internalization defect is merely due to a physical restriction in the formation of endocytic vesicles imposed by a change in sterol composition in the *ergΔ* mutant membranes. In support of this hypothesis, the removal of cholesterol from animal cells directly correlates with the flattening of clathrin-coated pits (Rodal *et al.*, 1999; Subtil *et al.*, 1999) and leads to a loss of the characteristic flask-shape morphology of caveolae (Rothberg *et al.*, 1990, 1992; Chang *et al.*, 1992; Hailstones *et al.*, 1998). Thus, cholesterol appears to affect the morphology and curvature of the plasma membrane in animal cells, and ergosterol may function in a similar manner in the yeast plasma membrane. At this point, however, we cannot exclude the possibility that ergosterol serves a combination of the proposed functions.

The present study identified sterols as a novel requirement for endocytosis in yeast. These results are consistent with the role of cholesterol in endocytosis in animal cells. The genetics of yeast, however, provide a powerful tool to understand the *in vivo* functions of specific portions of the ergosterol molecule in endocytosis. As shown here, the analysis of certain *ergΔ* mutants demonstrated that the desaturation state of the sterol B ring is crucial for the ability of sterols to function in the internalization step. In the future, a systematic analysis of other viable *ergΔ* single and double mutants that accumulate sterols with altered structural features should give a more defined view on how sterols function in endocytosis.

## ACKNOWLEDGMENTS

We thank the Riezman laboratory and in particular Dr. M. Isabel Geli, for stimulating discussions throughout the progression of this work and also thank Drs. Janet Lee and Mohan Balasubramanian for many comments and suggestions on the manuscript. We are grateful to Drs. F. Cvrckova and R. Gaber for sending strains and plasmids. We also thank Drs. Günther Daum and Dagmar Zweytkick for help with the sterol identification and Dr. Erich Leitner for help with

the GLC-MS. This work was funded by the Kanton Baselstadt and by grants to H.R. from the Swiss National Science Foundation and to A.H.-P. from the Human Frontier Science Program (LT-194/98) and the European Molecular Biology Organization (ASTF9273). During the completion of this work, A.L.M. was supported by the National Science and Technology Board of Singapore. H.P. was supported by the Fonds zur Förderung der wissenschaftlichen Forschung in Oesterreich (project 12076).

## REFERENCES

- Anderson, R.G. (1998). The caveolae membrane system. *Annu. Rev. Biochem.* *67*, 199–225.
- Arthington, B.A., Bennett, L.G., Skatrud, P.L., Guynn, C.J., Barbuch, R.J., Ulbright, C.E., and Bard, M. (1991). Cloning, disruption and sequence of the gene encoding yeast C-5 sterol desaturase. *Gene* *102*, 39–44.
- Bard, M., Woods, R.A., Barton, D.H., Corrie, J.E., and Widdowson, D.A. (1977). Sterol mutants of *Saccharomyces cerevisiae*: chromatographic analyses. *Lipids* *12*, 645–654.
- Bottema, C.D.K., McLean-Bowen, C.A., and Parks, L.W. (1983). Role of sterol structure in the thermotropic behavior of plasma membranes in *Saccharomyces cerevisiae*. *Biochim. Biophys. Acta* *734*, 235–248.
- Brown, D.A., and London, E. (1998). Functions of lipid rafts in biological membranes. *Annu. Rev. Cell Dev. Biol.* *14*, 111–136.
- Brown, R.E. (1998). Sphingolipid organization in biomembranes: what physical studies of model membranes reveal. *J. Cell Sci.* *111*, 1–9.
- Cerneus, D.P., Ueffing, E., Posthuma, G., Strous, G. J., and van der Ende, A. (1993). Detergent insolubility of alkaline phosphatase during biosynthetic transport and endocytosis. Role of cholesterol. *J. Biol. Chem.* *268*, 3150–3155.
- Chang, W.J., Rothberg, K.G., Kamen, B.A., and Anderson, R.G. (1992). Lowering the cholesterol content of MA104 cells inhibits receptor-mediated transport of folate. *J. Cell Biol.* *118*, 63–69.
- Chen, E.Y., and Seeburg, P.H. (1985). Supercoil sequencing: a fast and simple method for sequencing plasmid DNA. *DNA* *4*, 165–170.
- Daum, G., Lees, N.D., Bard, M., and Dickson, R. (1998). Biochemistry, cell biology and molecular biology of lipids of *Saccharomyces cerevisiae*. *Yeast* *14*, 1471–1510.
- Deckert, M., Tichioni, M., and Bernard, A. (1996). Endocytosis of GPI-anchored proteins in human lymphocytes: role of glycolipid-based domains, actin cytoskeleton, and protein kinases. *J. Cell Biol.* *133*, 791–799.
- Dickson, R.C. (1998). Sphingolipid functions in *Saccharomyces cerevisiae*: comparison to mammals. *Annu. Rev. Biochem.* *67*, 27–48.
- Dulic, V., Egerton, M., Elguindi, I., Raths, S., Singer, B., and Riezman, H. (1991). Yeast endocytosis assays. *Methods Enzymol.* *194*, 697–710.
- Fielding, C.J., and Fielding, P.E. (1997). Intracellular cholesterol transport. *J. Lipid Res.* *38*, 1503–1521.
- Folch, J., Lees, M., and Sloane Stanley, G.H. (1957). A simple method for the isolation and purification of total lipids from animal tissues. *J. Biol. Chem.* *226*, 497–509.
- Gaber, R.F., Copple, D.M., Kennedy, B.K., Vidal, M., and Bard, M. (1989). The yeast gene *ERG6* is required for normal membrane function but is not essential for biosynthesis of the cell-cycle-sparking sterol. *Mol. Cell. Biol.* *9*, 3447–3456.
- Geli, M.I., and Riezman, H. (1998). Endocytic internalization in yeast and animal cells: similar and different. *J. Cell Sci.* *111*, 1031–1037.
- Gietz, D., St. Jean, A., Woods, R.A., and Schiestl, R.H. (1992). Improved method for high efficiency transformation of intact yeast cells. *Nucleic Acids Res.* *20*, 1425.
- Gietz, R.D., and Sugino, A. (1988). New yeast-*Escherichia coli* shuttle vectors constructed with in vitro mutagenized yeast genes lacking six-bp restriction sites. *Gene* *74*, 527–534.
- Goldstein, A., and Lampen, J.O. (1975). Beta-D-fructofuranoside fructohydrolase from yeast. *Methods Enzymol.* *42*, 504–511.
- Hailstones, D., Sleer, L.S., Parton, R.G., and Stanley, K.K. (1998). Regulation of caveolin and caveolae by cholesterol in MDCK cells. *J. Lipid Res.* *39*, 369–379.
- Harder, T., and Simons, K. (1997). Caveolae, DIGs, and the dynamics of sphingolipid-cholesterol microdomains. *Curr. Opin. Cell Biol.* *9*, 534–542.
- Hardwick, K.G., and Pelham, H.R. (1994). *SED6* is identical to *ERG6*, and encodes a putative methyltransferase required for ergosterol synthesis. *Yeast* *10*, 265–269.
- Keesler, G.A., Casey, W.M., and Parks, L.W. (1992). Stimulation by heme of steryl ester synthase and aerobic sterol exclusion in the yeast *Saccharomyces cerevisiae*. *Arch. Biochem. Biophys.* *296*, 474–481.
- Klionsky, D.J., Herman, P.K., and Emr, S.D. (1990). The fungal vacuole: composition, function, and biogenesis. *Microbiol. Rev.* *54*, 266–292.
- Kobayashi, T., Gu, F., and Gruenberg, J. (1998). Lipids, lipid domains and lipid-protein interactions in endocytic membrane traffic. *Semin. Cell Dev. Biol.* *9*, 517–526.
- Kübler, E., Dohlman, H.G., and Lisanti, M.P. (1996). Identification of Triton X-100 insoluble membrane domains in the yeast *Saccharomyces cerevisiae*. Lipid requirements for targeting of heterotrimeric G-protein subunits. *J. Biol. Chem.* *271*, 32975–32980.
- Kübler, E., and Riezman, H. (1993). Actin and fimbrin are required for the internalization step of endocytosis in yeast. *EMBO J.* *12*, 2855–2862.
- Laemmli, U.K. (1970). Cleavage of structural proteins during the assembly of the head of bacteriophage T4. *Nature* *227*, 680–685.
- Lamaze, C., Fujimoto, L.M., Yin, H.L., and Schmid, S.L. (1997). The actin cytoskeleton is required for receptor-mediated endocytosis in mammalian cells. *J. Biol. Chem.* *272*, 20332–20335.
- Lange, Y. (1991). Disposition of intracellular cholesterol in human fibroblasts. *J. Lipid Res.* *32*, 329–339.
- Leber, A., Fischer, P., Schneider, R., Kohlwein, S.D., and Daum, G. (1997). The yeast *mic2* mutant is defective in the formation of mannosyl-diinositolphosphorylceramide. *FEBS Lett.* *411*, 211–214.
- Leber, R., Zinser, E., Hrastnik, C., Paltauf, F., and Daum, G. (1995). Export of steryl esters from lipid particles and release of free sterols in the yeast *Saccharomyces cerevisiae*. *Biochim. Biophys. Acta* *1234*, 119–126.
- Lees, N.D., Bard, M., Kemple, M.D., Haak, R.A., and Kleinhans, F.W. (1979). ESR determination of membrane order parameter in yeast sterol mutants. *Biochim. Biophys. Acta* *553*, 469–475.
- Lees, N.D., Skaggs, B., Kirsch, D.R., and Bard, M. (1995). Cloning of the late genes in the ergosterol biosynthetic pathway of *Saccharomyces cerevisiae*—a review. *Lipids* *30*, 221–226.
- Lewis, T.A., Rodriguez, R.J., and Parks, L.W. (1987). Relationship between intracellular sterol content and sterol esterification and hydrolysis in *Saccharomyces cerevisiae*. *Biochim. Biophys. Acta* *921*, 205–212.
- Lorenz, R.T., Casey, W.M., and Parks, L.W. (1989). Structural discrimination in the sparking function of sterols in the yeast *Saccharomyces cerevisiae*. *J. Bacteriol.* *171*, 6169–6173.



- Mellman, I. (1996). Endocytosis and molecular sorting. *Annu. Rev. Cell Dev. Biol.* 12, 575–625.
- Munn, A.L., and Riezman, H. (1994). Endocytosis is required for the growth of vacuolar H(+)-ATPase-defective yeast: identification of six new END genes. *J. Cell Biol.* 127, 373–386.
- Munn, A.L., Stevenson, B.J., Geli, M.I., and Riezman, H. (1995). end5, end6, and end7: mutations that cause actin delocalization and block the internalization step of endocytosis in *Saccharomyces cerevisiae*. *Mol. Biol. Cell* 6, 1721–1742.
- Nes, W.D., Janssen, G.G., Crumley, F.G., Kalinowska, M., and Akishita, T. (1993). The structural requirements of sterols for membrane function in *Saccharomyces cerevisiae*. *Arch. Biochem. Biophys.* 300, 724–733.
- Nes, W.D., Xu, S.H., and Haddon, W.F. (1989). Evidence for similarities and differences in the biosynthesis of fungal sterols. *Steroids* 53, 533–558.
- Novick, P., Ferro, S., and Schekman, R. (1981). Order of events in the yeast secretory pathway. *Cell* 25, 461–469.
- Novick, P., and Schekman, R. (1979). Secretion and cell-surface growth are blocked in a temperature-sensitive mutant of *Saccharomyces cerevisiae*. *Proc. Natl. Acad. Sci. USA* 76, 1858–1862.
- Orlandi, P.A., and Fishman, P.H. (1998). Filipin-dependent inhibition of cholera toxin: evidence for toxin internalization and activation through caveolae-like domains. *J. Cell Biol.* 141, 905–915.
- Parks, L.W., and Casey, W.M. (1995). Physiological implications of sterol biosynthesis in yeast. *Annu. Rev. Microbiol.* 49, 95–116.
- Parton, R.G., Joggerst, B., and Simons, K. (1994). Regulated internalization of caveolae. *J. Cell Biol.* 127, 1199–1215.
- Patterson, G.W. (1971). Relation between structure and retention time of sterols in gas chromatography. *Anal. Chem.* 43, 1165–1170.
- Raths, S., Rohrer, J., Crausaz, F., and Riezman, H. (1993). end3 and end4: two mutants defective in receptor-mediated and fluid-phase endocytosis in *Saccharomyces cerevisiae*. *J. Cell Biol.* 120, 55–65.
- Riezman, H. (1985). Endocytosis in yeast: several of the yeast secretory mutants are defective in endocytosis. *Cell* 40, 1001–1009.
- Riezman, H., Munn, A., Geli, M.I., and Hicke, L. (1996). Actin-, myosin- and ubiquitin-dependent endocytosis. *Experientia* 52, 1033–1041.
- Robinson, J.S., Klionsky, D.J., Banta, L.M., and Emr, S.D. (1988). Protein sorting in *Saccharomyces cerevisiae*: isolation of mutants defective in the delivery and processing of multiple vacuolar hydrolases. *Mol. Cell. Biol.* 8, 4936–4948.
- Rodal, S.K., Skretting, G., Garred, O., Vilhardt, F., van Deurs, B., and Sandvig, K. (1999). Extraction of cholesterol with methyl-beta-cyclodextrin perturbs formation of clathrin-coated endocytic vesicles. *Mol. Biol. Cell* 10, 961–974.
- Rodriguez, R.J., and Parks, L.W. (1983). Structural and physiological features of sterols necessary to satisfy bulk membrane and sparking requirements in yeast sterol auxotrophs. *Arch. Biochem. Biophys.* 225, 861–871.
- Rothberg, K.G., Heuser, J.E., Donzell, W.C., Ying, Y.S., Glenney, J.R., and Anderson, R.G. (1992). Caveolin, a protein component of caveolae membrane coats. *Cell* 68, 673–682.
- Rothberg, K.G., Ying, Y.S., Kamen, B.A., and Anderson, R.G. (1990). Cholesterol controls the clustering of the glycospholipid-anchored membrane receptor for 5-methyltetrahydrofolate. *J. Cell Biol.* 111, 2931–2938.
- Rothman, J.H., Hunter, C.P., Valls, L.A., and Stevens, T.H. (1986). Overproduction-induced mislocalization of a yeast vacuolar protein allows isolation of its structural gene. *Proc. Natl. Acad. Sci. USA* 83, 3248–3252.
- Sambrook, J., Fritsch, E.F., and Maniatis, T. (1989). *Molecular Cloning: A Laboratory Manual*, 2nd ed., Cold Spring Harbor, NY: Cold Spring Harbor Laboratory Press.
- Schnitzer, J.E., Oh, P., Pinney, E., and Allard, J. (1994). Filipin-sensitive caveolae-mediated transport in endothelium: reduced transcytosis, scavenger endocytosis, and capillary permeability of select macromolecules. *J. Cell Biol.* 127, 1217–1232.
- Sherman, F., Fink, G., and Lawrence, C. (1974). *Methods in Yeast Genetics*, Cold Spring Harbor, NY: Cold Spring Harbor Laboratory Press.
- Simons, K., and Ikonen, E. (1997). Functional rafts in cell membranes. *Nature* 387, 569–572.
- Stevens, T., Esmon, B., and Schekman, R. (1982). Early stages in the yeast secretory pathway are required for transport of carboxypeptidase Y to the vacuole. *Cell* 30, 439–448.
- Subtil, A., Gaidarov, I., Kobylarz, K., Lampson, M.A., Keen, J.H., and McGraw, T.E. (1999). Acute cholesterol depletion inhibits clathrin-coated pit budding. *Proc. Natl. Acad. Sci. USA* 96, 6775–6780.
- Tomeo, M.E., Fenner, G., Tove, S.R., and Parks, L.W. (1992). Effect of sterol alterations on conjugation in *Saccharomyces cerevisiae*. *Yeast* 8, 1015–1024.
- Trocha, P.J., and Sprinson, D.B. (1976). Location and regulation of early enzymes of sterol biosynthesis in yeast. *Arch. Biochem. Biophys.* 174, 45–51.
- van den Hazel, H.B., Pichler, H., do Valle Matta, M.A., Leitner, E., Goffeau, A., and Daum, G. (1999). PDR16 and PDR17, two homologous genes of *Saccharomyces cerevisiae*, affect lipid biosynthesis and resistance to multiple drugs. *J. Biol. Chem.* 274, 1934–1941.
- Ward, A.C. (1990). Single-step purification of shuttle vectors from yeast to high frequency back-transformation into *E. coli*. *Nucleic Acids Res.* 18, 5319.
- Welihinda, A.A., Beavis, A.D., and Trumbly, R.J. (1994). Mutations in LIS1 (ERG6) gene confer increased sodium and lithium uptake in *Saccharomyces cerevisiae*. *Biochim. Biophys. Acta* 1193, 107–117.
- Wendland, B., Emr, S.D., and Riezman, H. (1998). Protein traffic in the yeast endocytic and vacuolar protein sorting pathways. *Curr. Opin. Cell Biol.* 10, 513–522.
- Xu, S.H., Norton, R.A., Crumley, F.G., and Nes, W.D. (1988). Comparison of the chromatographic properties of sterols, select additional steroids and triterpenoids: gravity-flow column liquid chromatography, TLC, gas-liquid chromatography and high-performance liquid chromatography. *J. Chromatogr.* 452, 377–398.
- Zinser, E., Paltauf, F., and Daum, G. (1993). Sterol composition of yeast organelle membranes and subcellular distribution of enzymes involved in sterol metabolism. *J. Bacteriol.* 175, 2853–2858.